

# Reverse crosstalk of TGF $\beta$ and PPAR $\beta/\delta$ signaling identified by transcriptional profiling

Josefine Stockert, Till Adhikary, Kerstin Kaddatz, Florian Finkernagel, Wolfgang Meissner, Sabine Müller-Brüsselbach and Rolf Müller\*

Institute of Molecular Biology and Tumor Research (IMT), Philipps-University, Emil-Mannkopff-Strasse 2, 35032 Marburg, Germany

Received May 17, 2010; Revised August 11, 2010; Accepted August 14, 2010

## ABSTRACT

Previous work has provided strong evidence for a role of peroxisome proliferator-activated receptor  $\beta/\delta$  (PPAR $\beta/\delta$ ) and transforming growth factor- $\beta$  (TGF $\beta$ ) in inflammation and tumor stroma function, raising the possibility that both signaling pathways are interconnected. We have addressed this hypothesis by microarray analyses of human diploid fibroblasts induced to myofibroblastic differentiation, which revealed a substantial, mostly reverse crosstalk of both pathways and identified distinct classes of genes. A major class encompasses classical PPAR target genes, including *ANGPTL4*, *CPT1A*, *ADRP* and *PDK4*. These genes are repressed by TGF $\beta$ , which is counteracted by PPAR $\beta/\delta$  activation. This is mediated, at least in part, by the TGF $\beta$ -induced recruitment of the corepressor SMRT to PPAR response elements, and its release by PPAR $\beta/\delta$  ligands, indicating that TGF $\beta$  and PPAR $\beta/\delta$  signals are integrated by chromatin-associated complexes. A second class represents TGF $\beta$ -induced genes that are downregulated by PPAR $\beta/\delta$  agonists, exemplified by *CD274* and *IL6*, which is consistent with the anti-inflammatory properties of PPAR $\beta/\delta$  ligands. Finally, cooperative regulation by both ligands was observed for a minor group of genes, including several regulators of cell proliferation. These observations indicate that PPAR $\beta/\delta$  is able to influence the expression of distinct sets of both TGF $\beta$ -repressed and TGF $\beta$ -activated genes in both directions.

## INTRODUCTION

Peroxisome proliferator-activated receptors (PPARs) are nuclear receptors that function as ligand-inducible transcription factors (1–3). The three PPAR subtypes (PPAR $\alpha$ , PPAR $\beta/\delta$  and PPAR $\gamma$ ) activate their target genes through binding to PPAR response elements (PPREs) as heterodimers with members of the retinoid X receptor (RXR) family. PPARs play a central role in lipid metabolism by serving as sensors for fatty acids and fatty acid metabolites with major function as modulators of metabolic and inflammatory processes. Consequently, the transcriptional activity of PPARs is modulated not only by natural fatty acids, but also by lipid-derived metabolites such as prostaglandins J<sub>2</sub> and I<sub>2</sub>, leukotriene A<sub>4</sub>, 15-hydroxyeicosatetraenoic acid and 1-palmitoyl-2-oleoyl-sn-glycerol-3-phosphocholine (4–7). PPARs also play essential roles in developmental processes, wound healing, cell differentiation and proliferation and many associated diseases, including arteriosclerosis, diabetes, fibrosis, inflammatory disorders and cancer (8–12), which led to the development of numerous subtype-selective, high-affinity ligands (13).

We and others have shown that PPAR $\beta/\delta$  plays an essential role in regulating the differentiation, function and proliferation of tumor stroma cells (14–16). *Ppard*-null mice show gross alterations of tumor endothelial cells and fibroblasts, resulting in a high proportion of immature, dysfunctional microvessels and increased numbers of myofibroblastic cells (14). Consistent with these *in vivo* data, overexpression of PPAR $\beta/\delta$  inhibited the proliferation of cultured fibroblasts (14). Likewise, the prostacyclin mimetic Treprostinil inhibited the proliferation of lung fibroblasts concomitant with the transcriptional activation of PPAR $\beta/\delta$  (17). A regulatory role for PPAR $\beta/\delta$  in myofibroblasts has also been shown in a cell

\*To whom correspondence should be addressed. Tel: +49 6421 28 66236; Fax: +49 6421 28 68923; Email: rmueller@imt.uni-marburg.de

The authors wish it to be known that, in their opinion, the first two authors should be regarded as joint First Authors.

culture model of cardiac fibrosis, i.e. neonatal rat cardiac fibroblasts induced to myofibroblast transdifferentiation by culturing on a rigid substrate (18). Finally, different PPAR subtypes have been shown to play a role in experimentally induced lung fibrosis, and it has been suggested that PPAR $\beta/\delta$  agonists may attenuate disease progression by inhibiting myofibroblast proliferation and function (19).

A cytokine present in vast amounts in many tumors and playing a pivotal role in both tumor stroma function, inflammation and tissue fibrosis is the transforming growth factor- $\beta$  (TGF $\beta$ ) (20), suggesting that PPAR $\beta/\delta$  and TGF $\beta$  signaling pathways may functionally interact. To test this hypothesis, we performed microarray analyses of human lung fibroblasts induced to differentiate into myofibroblastic cells by TGF $\beta$  and analyzed the influence of PPAR $\beta/\delta$  agonists on the transcriptional profile. This study revealed an extensive, mainly reverse crosstalk of the transcriptional pathways regulated by PPAR $\beta/\delta$  and TGF $\beta$ , leading to the definition of distinct classes of genes. Class A genes are repressed by TGF $\beta$ , which is, at least in part, due to the induction of the corepressor SMRT and is counteracted by PPAR $\beta/\delta$  agonists. These include many known PPAR target genes with functions in lipid metabolism. A prominent example is the *ANGPTL4* gene, which encodes an important regulator of lipid metabolism and presumptive modulator of metastasis (21,22). In contrast, class B genes are induced by TGF $\beta$  and downregulated by PPAR $\beta/\delta$  agonists. These genes include *IL6*, which may be relevant in view of the reported anti-inflammatory and anti-fibrotic properties of PPAR $\beta/\delta$ .

## MATERIALS AND METHODS

### Chemicals

TGF $\beta$ 1 was purchased from Sigma-Aldrich (Karlsruhe, Germany), GW501516, GW1929 and GW7647 from Axxora (Lörrach, Germany), and L165,041 from Calbiochem (Merck, Darmstadt, Germany).

### Cell culture

WI-38 cells were obtained from the ATCC and maintained in DMEM/MCDB105 (1:1, PAA, Cölbe, Germany/Sigma, Steinheim, Germany) supplemented with 10% fetal bovine serum, 100 U/ml penicillin and 100  $\mu$ g/ml streptomycin in a humidified incubator at 37°C and 5% CO<sub>2</sub>. Differentiation by TGF $\beta$ 1 was carried out in serum-free medium as described (23,24).

### Immunostaining and quantification of stress fibers

Cells were fixed with ethanol (70%), stained by indirect immunofluorescence using a polyclonal  $\alpha$ -SMA antibody (Sigma, Steinheim, Germany) visualized by a Cy5-labeled secondary antibody (Molecular Probes A11029, Invitrogen, Karlsruhe, Germany), and counterstained with Hoechst 33258 (Invitrogen). Slides were evaluated with a Leica RMB 3 microscope equipped with fluorescence optics. For quantitative evaluation of SMA stress

fibers detected by immunofluorescence, cells showing strong, weak or no staining were counted separately. A total of  $\sim$ 750 cells in eight microscopic fields were counted per sample.

### Small-interfering RNA transfections

Cells were seeded at a density of  $5 \times 10^5$  cells per 6 cm dish in 4 ml DMEM with 10% fetal calf serum (FCS) and cultured for 2 h. 1280 ng small-interfering RNA (siRNA) in 100  $\mu$ l OptiMEM (Invitrogen) and 20  $\mu$ l HiPerfect (Qiagen, Hilden, Germany) were mixed and incubated for 5–10 min at room temperature prior to transfection. The cells were replated 24 h post-transfection at a density of  $5 \times 10^5$  cells per 6 cm dish. Transfection was repeated 48 h after start of the experiment, and cells were passaged after another 24 h. Forty-eight hours following the last transfection, cells were incubated in serum-free medium for 24 h before stimulation. The *NCOR2* siRNA pool was composed of the following sequences:

Hs\_NCOR2\_1: 5'-GGA CGG AGA UCU UCA AUA U;   
Hs\_NCOR2\_2: 5'-GAA CCU CGA UGA GAU CUU G;   
Hs\_NCOR2\_3: 5'-GGA AAA GAC UCA AAG UAA A;   
Hs\_NCOR2\_4: 5'-GCG CAC CUA UGA CAU GAU G;

control siRNA (#1022563, Qiagen, Hilden, Germany).

### Quantitative real-time polymerase chain reaction

Complementary DNA (cDNA) was synthesized from 0.1–1  $\mu$ g of RNA using oligo(dT) primers and the Omniscript kit (Qiagen, Hilden, Germany). Quantitative polymerase chain reaction (qPCR) was performed in a Mx3000P Real-Time PCR system (Stratagene, La Jolla, CA, USA) for 40 cycles at an annealing temperature of 60°C. PCR reactions were carried out using the Absolute QPCR SYBR Green Mix (Abgene, Hamburg, Germany) and a primer concentration of 0.2  $\mu$ M following the manufacturer's instructions. *L27* was used as normalizer. Comparative expression analyses were statistically analyzed by Student's *t*-test (two-tailed, equal variance) and Bonferroni correction. The sequences of the primers are as follows:

ANGPTL4fw: 5'-GATGGCTCAGTGGACTTCAACC;   
ANGPTL4rv: 5'-CCCGTGATGCTATGCACCTTC;   
L27fw: 5'-AAAGCCGTCATCGTGAAGAAC;   
L27rv: 5'-GCTGTCACTTTCCGGGGATAG;   
PPARDfw: 5'-TCATTGCGGCCATCATTCTGTGTG;   
PPARDrv: 5'-TTCGGTCTTCTTGATCCGCTGCAT;   
ADRPfw: 5'-TGTGAGATGGCAGAGAACGGT;   
ADRPrv: 5'-CTGCTCACGAGCTGCATCATC;   
CPT1Afw: 5'-ACAGTCGGTGAGGCCCTCTTATGAA;   
CPT1Arv: 5'-TCTTGCTGCCTGAATGTGAGTTGG;   
PDK4fw: 5'-TTGAGTGTTC AAGGATGCTCTG;   
PDK4rv: 5'-TGCCCGCATTGCATTCTTAAATA;   
COL4A1fw: 5'-ACTCTTTTGTGATGCACACCA;   
COL4A1rv: 5'-AAGCTGTAAGCGTTTTCGTA;   
ACTA2fw: 5'-TGATCACCATCGGAAATGAA;   
ACTA2rv: 5'-TGATGCTGTTGTAGGTGGTTTC;   
SM22Afw: 5'-TTGAAGGCAAAGACATGGCAG;   
SM22Arv: 5'-CCATCTGAAGGCCAATGACAT;

ANGPTL4fw: 5'-GATGGCTCAGTGGACTTCAACC;  
 ANGPTL4rv: 5'-CCCGTGATGCTATGCACCTTC;  
 L27fw: 5'-AAAGCCGTCATCGTGAAGAAC;  
 L27rv: 5'-GCTGTCACTTTCCGGGGATAG;  
 PPARdfw: 5'-TCATTGCGGCCATCATTCTGTGTG;  
 PPARdrv: 5'-TTCGGTCTTCTTGATCCGCTGCAT;  
 ADRPfw: 5'-TGTGAGATGGCAGAGAACGGT;  
 ADRPrv: 5'-CTGCTCACGAGCTGCATCATC;  
 CPT1Afw: 5'-ACAGTCGGTGAGGCCTCTTATGAA;  
 CPT1Arv: 5'-TCTTGCTGCCTGAATGTGAGTTGG;  
 PDK4fw: 5'-TTGAGTGTTCAAGGATGCTCTG;  
 PDK4rv: 5'-TGCCCGCATTGCATTCTTAAATA;  
 COL4A1fw: 5'-ACTCTTTGTGATGCACACCA;  
 COL4A1rv: 5'-AAGCTGTAAGCGTTTGCGTA;  
 ACTA2fw: 5'-TGATCACCATCGGAAATGAA;  
 ACTA2rv: 5'-TGATGCTGTTGTAGGTGGTTTC;  
 SM22Afw: 5'-TTGAAGGCAAAGACATGGCAG;  
 SM22Arv: 5'-CCATCTGAAGGCCAATGACAT;  
 CD274fw: 5'-GGCATCCAAGATACAAACTCAA;  
 CD274rv: 5'-CAGAAGTTCCAATGCTGGATTA;  
 CLDN1fw: 5'-CCCTATGACCCCAGTCAATG;  
 CLDN1rv: 5'-ACCTCCCAGAAGGCAGAGA;  
 IL6fw: 5'-CAGGAGCCCAGCTATGAACT;  
 IL6rv: 5'-AGCAGGCAACACCAGGAG;  
 NCOR1fw: 5'-TCGCTTCCACTGTTTCTGC;  
 NCOR1rv: 5'-GGGCTTGACAGCTTCAACTT;  
 NCOR2fw: 5'-CGGAGTGACCACACTCAC;  
 NCOR2rv: 5'-GGGTCTGCCAGAGACCTTG.

### Chromatin immunoprecipitation

Chromatin immunoprecipitation (ChIP) was performed as described (6), except that nuclei were resuspended at  $2.5 \times 10^7$ /ml, and 60 pulses were applied during sonication. The following antibodies were used: IgG pool, I5006 (Sigma-Aldrich, Steinheim, Germany),  $\alpha$ -PPAR $\beta/\delta$ , sc-7197 (Santa Cruz, Heidelberg, Germany);  $\alpha$ -SMRT, ab24551 (Abcam, Cambridge, UK). Comparative binding analyses were statistically analyzed by Student's *t*-test (two-tailed, equal variance) and corrected for multiple hypothesis testing by the Bonferroni method. Primer sequences were as follows:

ANGPTL4+3500fw: 5'-CCTTACTGGATGGGAGGAAAG;  
 ANGPTL4+3500rv: 5'-CCCAGAGTGACCAGGAAGAC;  
 ANGPTL4-12000fw: 5'-ACCCTGGGTGTTTCATGGTAG;  
 ANGPTL4-12000rv: 5'-CCCAAGGGGTTCAATGTATTC.

### Microarrays

RNA was isolated using the Nucleospin RNA II kit (Macherey-Nagel, Düren, Germany). RNA quality was assessed using the Experion automated electrophoresis station with RNA StdSens chips (Bio-Rad, Munich, Germany). For microarray studies, total RNA samples were amplified and labeled using the Agilent Quick Amp Labeling Kit (Agilent, Santa Clara, CA, USA) according to the manufacturer's instructions. The amplification procedure consists of reverse transcription of total RNA, including spike-in with an oligo(dT) primer bearing a T7 promoter, followed by *in vitro* transcription of the

resulting cDNA with T7 RNA polymerase in the presence of dye labeled CTP to generate multiple fluorescence labeled copies of each messenger RNA (mRNA). After purification, the labeled aRNA was quantified and hybridization samples were prepared according to the manufacturer's instructions. Human Agilent 4-plex Array 44K were used for the analysis of the gene expression of the different samples in a reference-design assay. As a reference, a pool of all samples was used. This reference was labeled with Cy3, while the samples were labeled with Cy5 dye. The hybridization assembly was performed as described in the *Agilent Microarray Hybridization Chamber User Guide* (G2534-90001). After a 17-h hybridization at 65°C, slides were washed as described by the manufacturer and subsequently scanned using an Agilent DNA Microarray Scanner G2505C; scan software: Agilent Scan Control Version A.8.1.3; quantification software: Agilent Feature Extraction Version 10.5.1.1 (FE Protocol GE\_105\_Dec08). Raw microarray data were normalized using the 'loess' method implemented within the marray package of R/BioConductor ([www.bioconductor.org](http://www.bioconductor.org)). Regulated probes were selected on the basis that the logarithmic (base 2) average intensity value was  $\geq 6$ , and that the fluctuation between replicates was  $\leq 50\%$ .

## RESULTS

### Induction of myofibroblastic differentiation of diploid human fibroblasts

The purpose of the present study was to investigate whether PPAR $\beta/\delta$  and TGF $\beta$  signaling pathways functionally interact. As an experimental model, we used diploid human lung fibroblasts (WI38 cells) induced by TGF $\beta$  to differentiate into myofibroblast-like cells. In order to characterize this system, we first studied the expression of the myofibroblast marker genes *ACTA2* (coding for smooth muscle  $\alpha$ -actin; SMA), *COL4A1* (encoding collagen type IV  $\alpha 1$ ) and *SM22A* (coding for smooth muscle protein 22- $\alpha$ ). As shown in Figure 1A and B, TGF $\beta$  induced the expression all three genes. Increased levels of *ACTA2* and *COL4A1* mRNA were detectable after 6 h and reached maximum levels after 24–36 h (Figure 1A). In the same experimental setup, no significant effect of the PPAR $\beta/\delta$  agonists GW501516 or L165,041 on the TGF $\beta$ -mediated induction of *ACTA2*, *COL4A1* and *SM22A* was detectable (Figure 1B), suggesting that the ligand-mediated activation of PPAR $\beta/\delta$  does not affect the myofibroblastic differentiation of WI38 cells.

Concomitantly with the induction of these marker genes, SMA-containing stress fibers, a hallmark of differentiating myofibroblasts, were readily detectable after 24 h exposure of WI38 cells to TGF $\beta$  (Figure 1C). Consistent with the marker gene expression data in Figure 1B, treatment with the PPAR $\beta/\delta$  agonist GW501516 had no detectable effect on stress fiber formation by TGF $\beta$  (Figure 1D).

As the deletion of *Ppard* in mice has been associated with myofibroblastic differentiation in the tumor stroma, we also investigated whether the inhibition of PPAR $\beta/\delta$



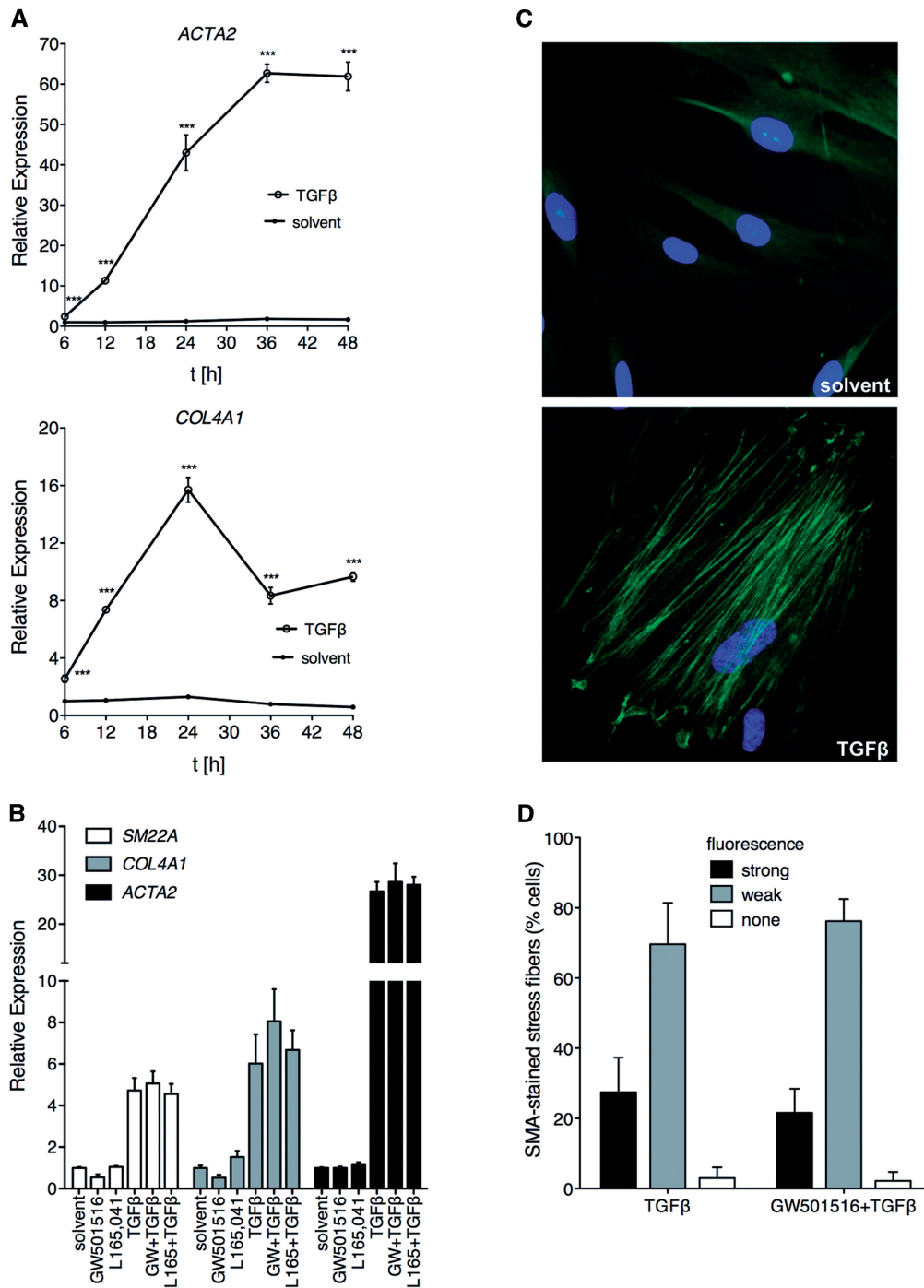


**Figure 1.** TGFβ-induced myofibroblast-like differentiation of WI38 cells is not affected by PPARβ/δ ligands. (A) Cells were treated with TGFβ1 (2 ng/ml) or solvent for the indicated times, and the relative expression levels of *ACTA2* and *COL4A1* were determined by RT-qPCR. \*\*\*, significant difference to solvent-treated sample ( $P < 0.001$  by *t*-test). (B) Expression of *ACTA2*, *COL4A1* and *SM22A* after 24h treatment with TGFβ1 (2 ng/ml), GW501516 (0.3 μM), L165,041 (2 μM), TGFβ1 plus PPARβ/δ ligand (as indicated) or solvent determined by RT-qPCR. No significant differences were detectable (*t*-test,  $P > 0.1$ ) in PPARβ/δ ligand-treated cells in either the absence or presence of TGFβ. (C) Staining by indirect immunofluorescence of SMA stress fibers (green) in WI38 cells treated with solvent or TGFβ for 24h as in (A). Nuclei were visualized by Hoechst 33258 staining (blue). (D) Quantitative evaluation of SMA fibers stained by immunofluorescence after treatment of WI38 cells with TGFβ or TGFβ plus GW501516 for 24h. Cells showing strong, weak or no staining were counted separately. For both samples, a total of 1500 cells in 16 microscopic fields were counted. Error bars represent the standard deviation for individual field counts.

expression in WI38 cells might affect the differentiation status of these cells. Supplementary Figure S1 shows that *ACTA2* expression indeed increased after the siRNA-mediated knockdown of PPARβ/δ. Taken

together, these observations suggest that PPARβ/δ plays a role in preventing myofibroblastic transdifferentiation under basal conditions, but that its activation by ligands does not prevent TGFβ-induced differentiation.

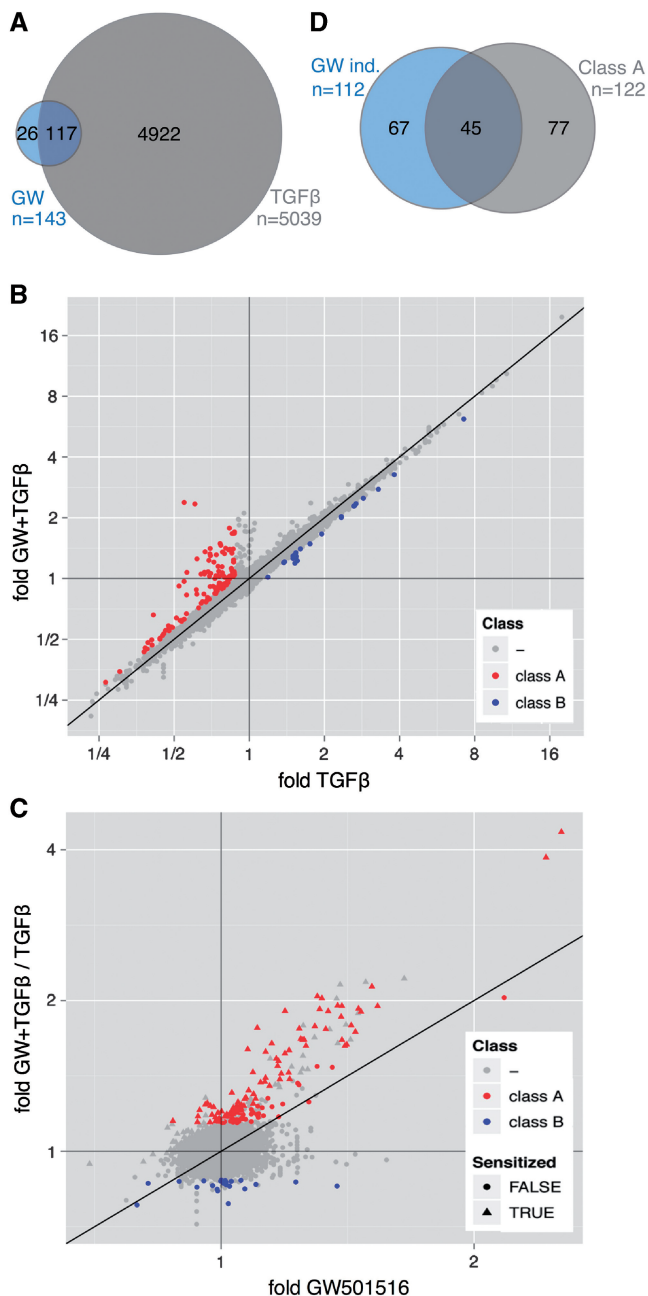


**Figure 2.** Genome-wide expression profiling of WI38 cells treated with TGFβ, PPARβ/δ agonist or both ligands. (A) Venn diagram depicting the numbers of probes showing regulation by TGFβ or GW501516 ( $\geq 1.3$ -fold change). The overlap represents those probes that indicate regulation by both ligands. (B) Dot plot analyzing for individual probes the effect of GW501516 on TGFβ-mediated regulation. Relative expression levels measured after co-treatment of WI38 cells with TGFβ plus GW501516 were plotted against expression levels measured after treatment with TGFβ alone. Red data points represent probes indicating reversion by GW501516 of TGFβ-mediated repression ( $\geq 1.3$ -fold upregulation; class A genes), blue data points represent probes indicating reversion by GW501516 of TGFβ-mediated activation ( $\geq 1.3$ -fold difference; class B genes). (C) Dot plot showing for individual probes a TGFβ-mediated increased GW501516 inducibility. Induction by GW501516 in the presence of TGFβ was plotted against the induction by GW501516 in the absence of TGFβ. The former value was calculated as the ratio of (fold induction by both ligands) / (fold induction by TGFβ). Red data points represent the class A probes defined in panel B. Triangles indicate sensitization by TGFβ, i.e. an increased induction ( $\geq 1.3$ -fold) by GW501516 in the

### Genome-wide expression profiling of WI38 cells treated with TGFβ and PPARβ/δ agonist

The fact that PPARβ/δ ligands do not affect the TGFβ-induced differentiation of WI38 cells makes this experimental system suitable to study possible interactions of these signaling pathways in myofibroblasts without interference by an altered differentiation state. Such interactions could, for instance, affect the functional activation or metabolic activity of these cells. We therefore used this model to address two questions: (i) does TGFβ alter the regulation of PPARβ/δ target genes, and (ii) do PPARβ/δ ligands impinge on TGFβ-mediated transcriptional signaling events that are associated with, for instance, inflammatory or fibrotic responses.

To identify potential functional interactions between TGFβ and PPARβ/δ signaling pathways, we performed microarray analyses of WI38 cells, either untreated (solvent) or treated with GW501516 (0.3 μM), TGFβ1 (2 ng/ml) or both ligands for 24 h (EMBL-EBI ArrayExpress, accession number E-MEXP-2750). As illustrated by the Venn diagram in Figure 2A, 5039 probes indicated regulation by TGFβ and 143 probes regulation by GW501516 ( $\geq 1.3$ -fold change) with an overlap of 117 probes. These correspond to 74 different annotated genes regulated by both ligands.

To determine cooperative or antagonistic effects exerted by TGFβ and GW501516, we compared for individual genes the transcriptional outcome of exposing WI38 cells to both ligands to that of treatment with either ligand alone, as described in the following sections.

### Modulation of TGFβ signaling by PPARβ/δ

The effect of GW501516 on TGFβ-mediated regulation was determined by plotting the relative expression levels measured after co-treatment with both ligands against the expression levels measured after treatment with TGFβ alone. The dot plot in Figure 2B identifies different set of probes showing distinct responses to TGFβ and GW501516.

'Class A' probes, which represent the major group defined in the present study, indicate repression by TGFβ that is counteracted by GW501516. This pattern was observed for a total of 136 probes, including 122 different annotated genes (cutoff  $\geq 1.3$ -fold upregulation by GW501516; red data points in Figure 2B; Supplementary Table S1). The characteristic expression pattern of class A genes in response to TGFβ and GW501516 is shown in Figure 3A, and validated by RT-qPCR (Figure 4) for *ANGPTL4* (angiopoietin-like 4), *PDK4* (pyruvate dehydrogenase kinase 4), *CPT1A* (carnitine palmitoyltransferase 1A) and *ADRP* (adipose differentiation-related protein). Several representative genes of this class are listed in Table 1.

presence of TGFβ ( $y$ -value/ $x$ -value  $\geq 1.3$ ). (D) Venn diagram illustrating the overlap between class A genes and all genes induced by GW501516 ( $\geq 30\%$  induction,  $n = 112$ ). This analysis includes only those genes, for which the effect of TGFβ could be evaluated in a statistically meaningful way. Therefore, the number of GW501516-induced genes is higher in (A).

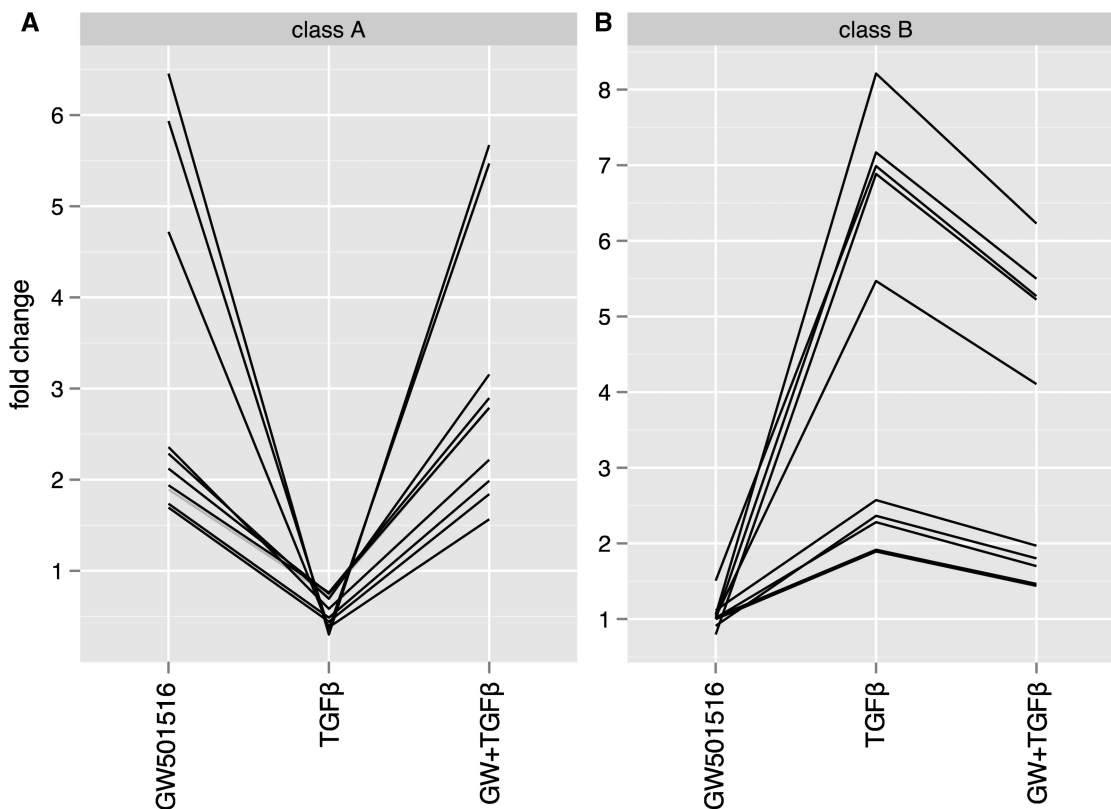


**Figure 3.** Graphic representation of the reverse effects of GW501516 on TGF $\beta$ -mediated gene regulation. The graphics show the expression patterns for the top 10 class A and class B genes identified in Figure 2B. (A) Repression by TGF $\beta$  counteracted by GW501516 (class A genes); (B) induction by TGF $\beta$  counteracted by GW501516 (class B genes).

'Class B' probes indicate a counteractive effect of GW501516 on TGF $\beta$ -mediated activation. This class encompasses 22 probes, representing 21 annotated genes (cutoff  $\geq 1.3$ -fold difference for TGF $\beta$  plus GW501516 relative to TGF $\beta$  alone; blue data points in Figure 2B; Supplementary Table S1). Their characteristic expression pattern in response to TGF $\beta$  and GW501516 is shown in Figure 3B. The RT-qPCR data in Figure 5 confirm that PPAR $\beta/\delta$  activation counteracts the TGF $\beta$ -mediated induction of the class B genes *IL6* (interleukin-6), *CD274* (B7-H1) and *CLDN1* (claudin 1), which was clearly detectable 6 h after application of GW501516, pointing to a direct effect of the PPAR $\beta/\delta$  ligands. No effect on the TGF $\beta$ -mediated induction of *IL6* was seen with the PPAR $\gamma$  ligand GW1929 or the PPAR $\alpha$  agonist GW7647 (Figure 5D), suggesting that the observed effect is PPAR $\beta/\delta$ -specific.

Cooperative regulation was also detectable for several probes (Figure 2B; not highlighted; class C and D in Supplementary Table S1), suggesting that GW501516 is able to influence the expression of distinct sets of both TGF $\beta$ -repressed and TGF $\beta$ -activated genes in both directions. Class C includes *KIT*, *FOXQ1* and *TOP2A*, which code for the tyrosine kinase receptor *KIT*, the transcription factor forkhead box Q1 and topoisomerase II, respectively. All three genes have been associated with cell cycle progression and tumorigenesis and may thus be of particular interest with respect to the function of TGF $\beta$  and PPAR $\beta/\delta$  in tumor and tumor stroma cells.

### Repression of PPAR $\beta/\delta$ target genes by TGF $\beta$ and counter-regulation by GW501516

We next determined for individual probes the effect of TGF $\beta$  on GW501516 inducibility. This was achieved by plotting the induction by GW501516 in the presence of TGF $\beta$  (fold GW501516 plus TGF $\beta$ /TGF $\beta$  alone) against the induction by GW501516 in the absence of TGF $\beta$  (Figure 2C). The predominant probe set identified by this analysis indicates increased induction ( $\geq 1.3$ -fold) by GW501516 in the presence of TGF $\beta$  (shown as triangles in Figure 2C). Surprisingly, a substantial number of these probes are identical to those showing repression by TGF $\beta$  and counter-regulation by GW501516 (red data points in Figure 2B and C). This overlap (Figure 2D) includes 37% of all class A probes (45/122) and 40% of all GW501516-induced sequences (45/112). The concomitant sensitization by TGF $\beta$  to activation by PPAR $\beta/\delta$  agonists and the reversal of the repressive effect of TGF $\beta$  by these ligands is also illustrated by the data in Figure 4 and Table 1. These findings suggest that the TGF $\beta$ -mediated repression of class A genes and its reversal by PPAR $\beta/\delta$  agonists are functionally linked.

### Enhancement of corepressor recruitment to PPAR response elements by TGF $\beta$

Finally, we addressed the molecular mechanisms that contribute to the regulation of class A genes. The activating and repressive activities of PPARs have been linked to

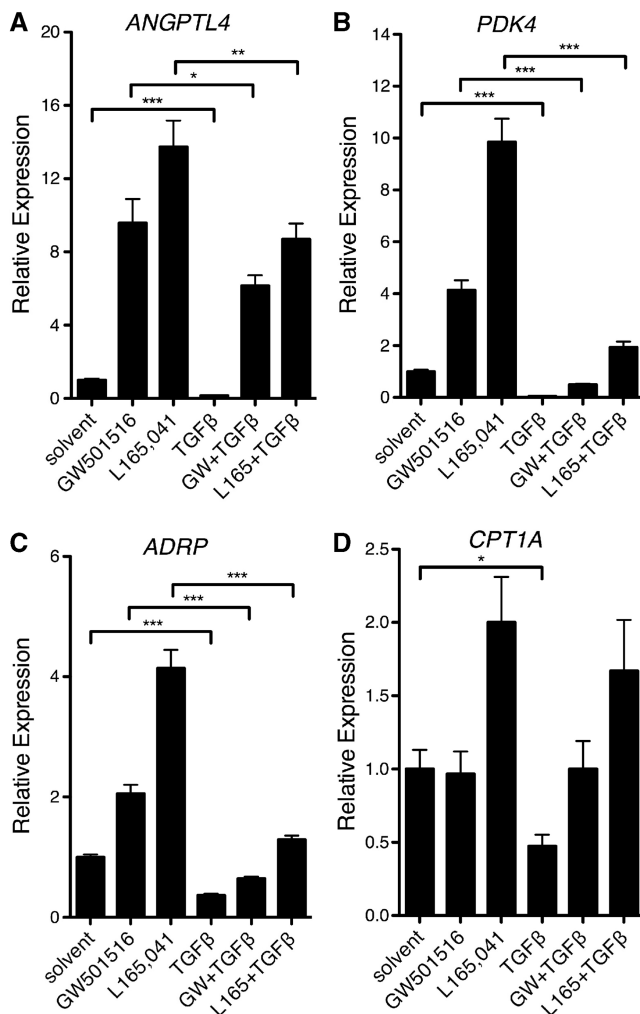


**Figure 4.** PPAR $\beta/\delta$  counteracts TGF $\beta$ -mediated transcriptional repression for a subgroup of target genes. Treatment of WI38 cells with TGF $\beta$  and/or PPAR $\beta/\delta$  ligands for 24 h and RT-qPCR analyses of *ANGPTL4* (A), *PDK4* (B), *ADRP* (C) and *CPT1A* (D) expression were performed as in Figure 1B. \*\*\*, \*\*, \* significant difference ( $P < 0.001$  by  $t$ -test,  $P < 0.01$ ,  $P < 0.05$ ).

interactions with proteins that serve as coactivators or corepressors, which in turn have profound effects on the local chromatin structure (9,25). Analysis of our microarray revealed a higher expression of several genes encoding corepressors of nuclear receptors in TGF $\beta$ -treated cells relative to solvent controls. These include *NCOR1* (coding for NCOR), *NCOR2* (encoding SMRT), *SHARP*, *LCOR*, *SIN3B*, *MTA1* and *CALR* (Figure 6A). Previous work by several laboratories has established a role for the corepressors NCOR and SMRT in transcriptional repression by unliganded PPAR $\beta/\delta$  *in vivo* (9,25–28). Upregulation of *NCOR2* was observed in RT-qPCR experiments already 6 h after treatment with TGF $\beta$ , whereas the induction of *NCOR1* was statistically not significant at this time point (Figure 6B).

We therefore analyzed whether TGF $\beta$  might influence the recruitment of SMRT to the PPREs of the *ANGPTL4* gene *in vivo*. Figure 6C shows that this is indeed the case. TGF $\beta$  treatment induced a 2.2-fold enhanced recruitment relative to solvent-treated cells, which was decreased to 1.3-fold in the presence of GW501516. This correlates well with the observed changes in *ANGPTL4* expression, pointing to a causal relationship between the regulation of class A genes and the recruitment of SMRT in response to TGF $\beta$  and GW501516.

To test this hypothesis, we analyzed the impact of *NCOR2* siRNA interference on TGF $\beta$  and GW501516-regulated *ANGPTL4* and *PDK4* gene expression. As shown in Figure 7A (left), the treatment of WI38 cells with *NCOR2* siRNA reduced *NCOR2* expression to 28–46% relative to cells exposed to control siRNA. The same treatment also attenuated the TGF $\beta$ -mediated repression of both PPAR target genes, whose relative expression levels increased in *NCOR2* siRNA-treated cells from 0.23 to 0.50 for *ANGPTL4*, and from 0.16 to 0.40 for *PDK4* (Figure 7A and B), respectively. This increased basal level expression was paralleled by a decreased inducibility by PPAR $\beta/\delta$  ligands in the presence of TGF $\beta$ , which dropped by ~50% for both genes (Figure 7A and C). The fact that similar patterns

**Table 1.** Representative examples of PPAR $\beta/\delta$  target genes regulated by TGF $\beta$ -mediated repression and reversal by GW501516 (class A genes)

Gene	Gene product	TGF $\beta^a$	GW501516 <sup>a</sup>	(GW501516 + TGF $\beta$ ) / TGF $\beta^b$
<i>ANGPTL4</i>	Angiopoietin-like 4	0.3	6.5	18.9
<i>PDK4</i>	Pyruvate dehydrogenase kinase, isozyme 4	0.4	4.7	4.1
<i>CPT1A</i>	Carnitine palmitoyltransferase 1A	0.5	2.0	3.2
<i>DDEF1IT1</i>	DDEF1 intronic transcript 1	0.7	1.5	2.8
<i>GPR137B</i>	G-protein-coupled receptor 137B	0.4	1.6	2.6
<i>SP100</i>	SP100 nuclear antigen	0.5	1.3	2.5
<i>SRGAP1</i>	SLIT-ROBO Rho GTPase activating protein 1	0.5	1.4	2.3
<i>IMPA2</i>	Inositol(myo)-1(or 4)-monophosphatase 2	0.3	1.7	2.2
<i>ACAA2</i>	Acetyl-Coenzyme A acyltransferase 2	0.7	1.4	2.0
<i>ABCA1</i>	ATP-binding cassette, sub-family A, member 1 (cholesterol transporter)	0.6	1.5	1.9
<i>ADRP</i>	Adipose differentiation-related protein	0.4	1.8	1.9
<i>CAT</i>	Catalase	0.4	1.5	1.8

<sup>a</sup>Relative expression values derived from microarray data (fold induction relative to solvent-treated cells).

<sup>b</sup>Values reflect GW501516-mediated induction in the presence of TGF $\beta$  corrected for the TGF $\beta$  effect.



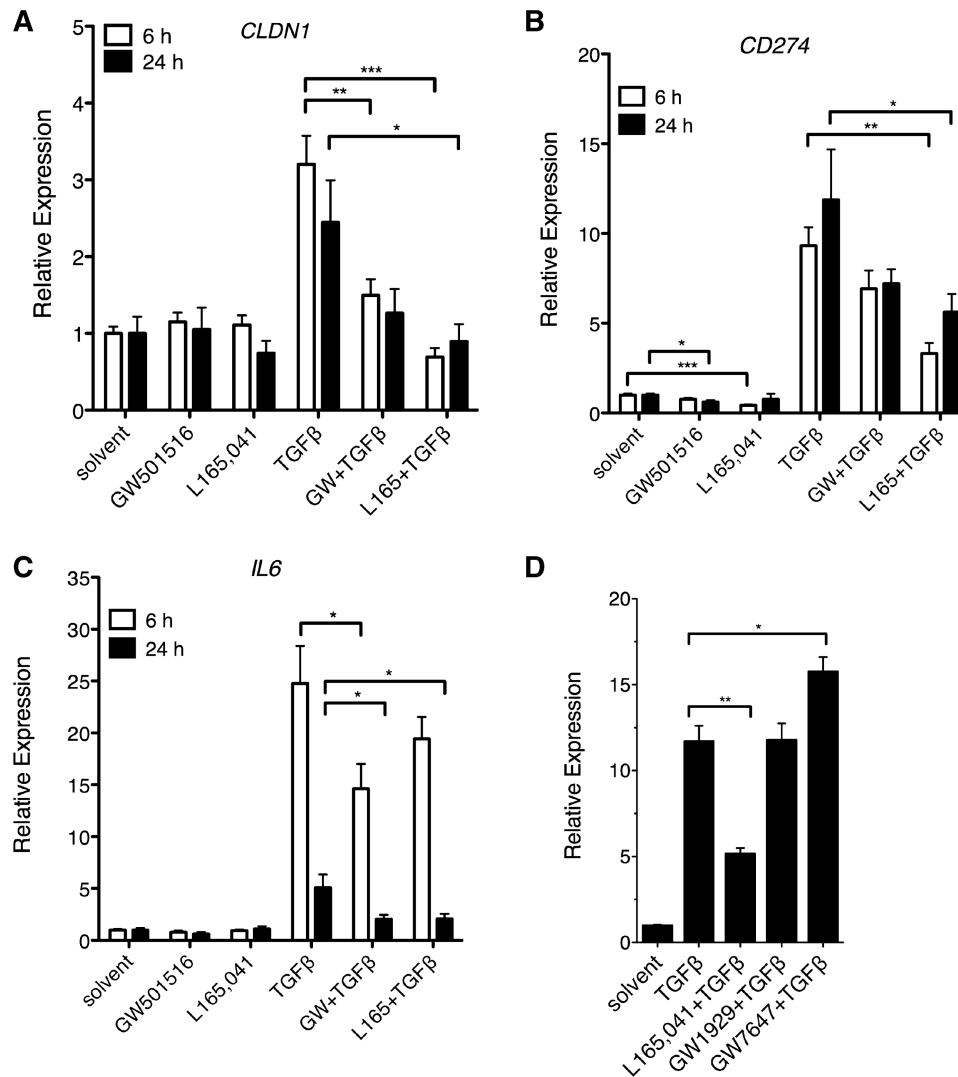


**Figure 5.** PPAR $\beta/\delta$  agonists inhibit TGF $\beta$ -mediated transcriptional activation for a subgroup of target genes. WI38 cells were treated with the PPAR $\beta/\delta$  ligands GW501516 and L165,041 for 16 h, subsequently stimulated with TGF $\beta$  for 6 or 24 h, and *CLDN1* (A), *CD274* (B) and *IL6* (C) expression was analyzed by RT-qPCR. (D) Comparison of the effects of the PPAR $\beta/\delta$  ligand L165,041, the PPAR $\gamma$  ligand GW1929 and the PPAR $\alpha$  agonist GW7647 on TGF $\beta$ -mediated induction of *IL6*. \*\*\*, \*\*, \* significant difference ( $P < 0.001$  by *t*-test,  $P < 0.01$ ,  $P < 0.05$ ).

were seen with both *ANGPTL4* and *PDK4* indicates that the regulatory mechanism identified in this study is not gene-specific. Taken together, these observations clearly establish a functional connection between SMRT, TGF $\beta$  and the transcription of PPAR $\beta/\delta$  target genes.

## DISCUSSION

Several lines of evidence strongly suggest that PPAR $\beta/\delta$  plays a role in regulating the differentiation and function of tumor stroma and inflammatory cells, pointing to a crosstalk of PPAR $\beta/\delta$  and cytokine signaling pathways. A cytokine with a pivotal function in inflammation and tumorigenesis is TGF $\beta$ . In the present study, we tested this hypothesis by asking whether PPAR $\beta/\delta$  and TGF $\beta$  signaling pathways functionally interact and modulate the transcriptional activity of common target genes in diploid

human fibroblasts induced to differentiate into myofibroblast-like cells.

### Reverse crosstalk of TGF $\beta$ and PPAR $\beta/\delta$ signaling

The potential interaction of transcriptional signaling pathways regulated by PPAR $\beta/\delta$  and TGF $\beta$  was analyzed by determining the genome-wide transcriptional profile of WI38 cells treated with TGF $\beta$ , a PPAR $\beta/\delta$  agonist or both ligands. The data obtained from this analysis point to an extensive crosstalk of the transcriptional signaling pathways regulated by PPAR $\beta/\delta$  and TGF $\beta$  (Figures 2 and 3). Bioinformatic analyses identified several classes of genes showing distinct responses to the combined action of TGF $\beta$  and PPAR $\beta/\delta$  agonists. Two of these classes that are of particular interest are characterized by the following distinct features (Figures 2B and 3): (i) repression by TGF $\beta$ , which is counteracted by PPAR $\beta/\delta$  agonists (class A genes; Table 1),



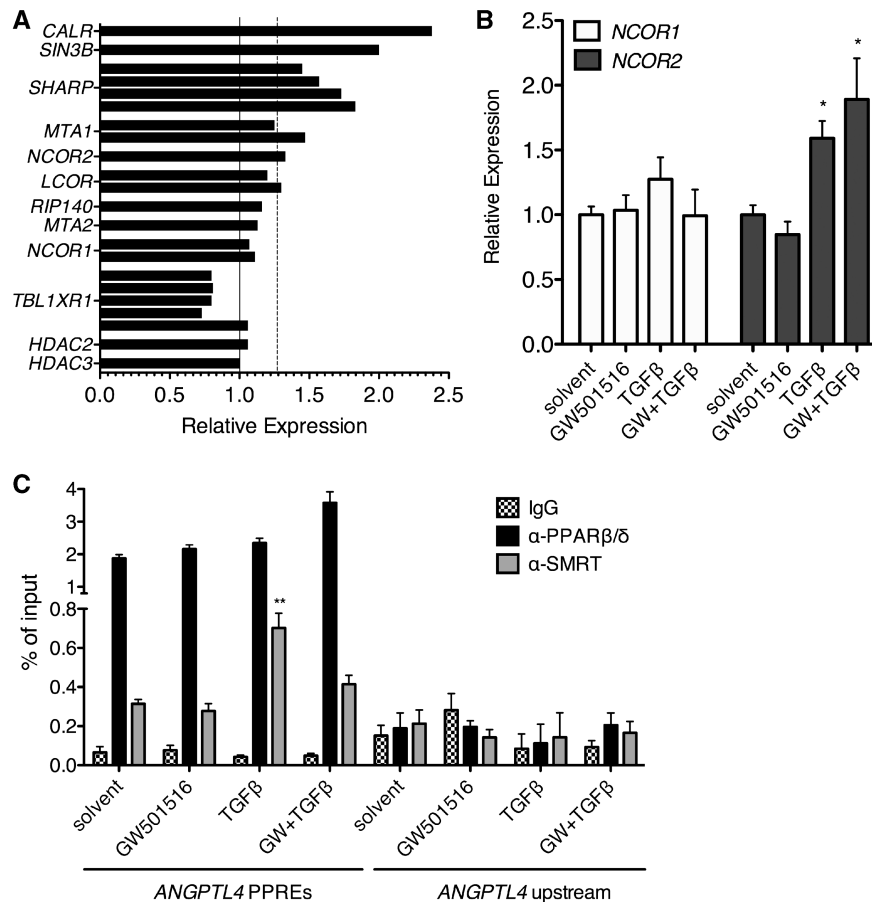


**Figure 6.** TGF $\beta$  induces corepressor expression and recruitment to the PPRE enhancer of the *ANGPTL4* gene *in vivo*. (A) Microarray data were analyzed for TGF $\beta$ -mediated effects on potential corepressor genes and plotted as relative expression values (TGF $\beta$  treatment versus solvent control). The dashed line denotes a threshold of 1.3-fold induction. (B) RT-qPCR analysis of *NCOR1* and *SMRT* expression 6 h following treatment of WI38 cells with GW501516, TGF $\beta$ 1 or both ligands. (C) TGF $\beta$  induces SMRT recruitment to the *ANGPTL4* PPRE enhancer *in vivo*. WI38 cells were treated with 0.3  $\mu$ M GW501516, 2 ng/ml TGF $\beta$ 1, or both for 24 h, and ChIP was carried out with antibodies against PPAR $\beta/\delta$ , SMRT or a nonspecific IgG pool, and an *ANGPTL4* region containing the PPRE enhancer (+3500 bp relative to the transcription start site) was amplified by qPCR. An *ANGPTL4* upstream region was included as a control. Signals were calculated relative to 1% of input DNA. \*\*, \* significant difference to solvent-treated sample ( $P < 0.01$  by *t*-test,  $P < 0.05$ ).

and (ii) induction by TGF $\beta$ , which is counteracted by PPAR $\beta/\delta$  agonists (class B genes). In both cases, PPAR $\beta/\delta$  agonists significantly inhibited the effect of TGF $\beta$ , indicating that this mode of interaction is a major feature of the interaction of these pathways.

#### Repression of PPAR $\beta/\delta$ target genes by TGF $\beta$ and reversal by GW501516

We also determined for individual probes the effect of TGF $\beta$  on ligand-mediated PPAR $\beta/\delta$  activation. This analysis identified a major set of genes, representing mostly classical PPAR target genes, such as *ANGPTL4*, *PDK4*, *ADRP* and *CPT1A*, which show increased induction by GW501516 in the presence of TGF $\beta$  (Figure 2C). These genes overlap to a large extent (37%) with class A genes (red data points in Figure 2B and C), indicating that the enhancement of GW501516 inducibility by TGF $\beta$  is functionally linked to their repression by TGF $\beta$ .

It has previously been shown that the *ANGPTL4* gene is induced by TGF $\beta$  in human breast cancer cell lines (21), which is in apparent contrast to the findings reported in

the present study. It is, however, well established that TGF $\beta$  frequently exerts opposite effects on target gene expression in mesenchymal and epithelial cells, and that neoplastic transformation can subvert TGF $\beta$ -mediated transcriptional regulation (29). It would thus be conceivable that the *ANGPTL4* gene is also subject to a similarly complex regulatory network. Consistent with this hypothesis is our observation (30) that *ANGPTL4* transcription is induced by TGF $\beta$  in the epithelial cell line HaCaT (31) and in WPMY-1 cells, which is a SV40-transformed cell line derived from human prostate carcinoma-associated fibroblasts (32). These findings suggest that the *ANGPTL4* gene is a useful model to investigate the molecular mechanisms underlying the cell type-specific and transformation-dependent effects of TGF $\beta$ -triggered transcriptional signaling pathways.

#### Correlation of the TGF $\beta$ /GW501516-mediated crosstalk with recruitment of the transcriptional corepressor SMRT

In the absence of ligands, PPAR $\beta/\delta$  target genes can be repressed through the recruitment of corepressors to

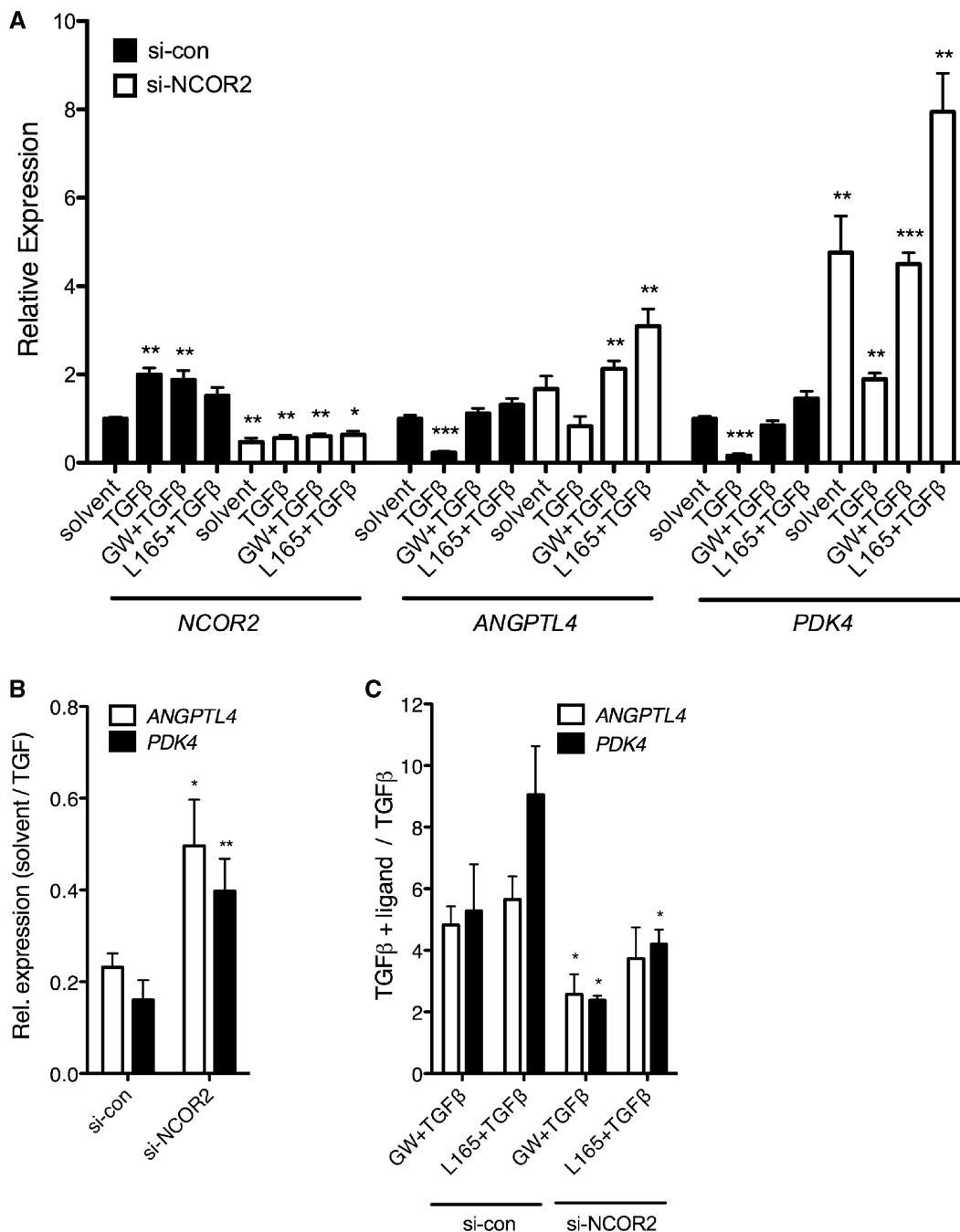


**Figure 7.** *NCOR2* induction plays a role in the TGF $\beta$ -triggered repression of PPAR $\beta/\delta$  target genes. (A) WI38 cells were transfected with *NCOR2* or control siRNA as described in 'Materials and Methods' section. Twenty-four hours after serum deprivation the cells were treated with TGF $\beta$ 1 (2 ng/ml), TGF $\beta$ 1 + GW501516 (0.3  $\mu$ M), TGF $\beta$ 1 + L165,041 (2  $\mu$ M) or solvent for 10 h, and *NCOR2*, *ANGPTL4* and *PDK4* mRNA levels were measured by RT-qPCR. The lower inducibility by GW501516 as compared to Figure 4 is presumably due to different cell densities and the siRNA treatment. (B) Effect of siRNA treatment on TGF $\beta$ -mediated *ANGPTL4* and *PDK4* repression. Values represent the ratio of expression levels in solvent-treated cells relative to TGF $\beta$ -treated cells. Experimental details as in (A). (C) Effect of siRNA treatment on PPAR $\beta/\delta$  ligand-mediated *ANGPTL4* and *PDK4* induction in the presence of TGF $\beta$ . Values represent the ratio of expression levels in cells treated with PPAR $\beta/\delta$  ligands plus TGF $\beta$  relative to TGF $\beta$ -treated cells. Experimental details as in (A). \*\*\*, \*\*, \* significant difference to solvent-treated (A) or si-con (B, C) sample ( $P < 0.001$  by *t*-test,  $P < 0.01$ ,  $P < 0.05$ ).

PPRE-bound PPAR $\beta/\delta$ -RXR heterodimers, such as NCOR and SMRT (9,25–28). In the present study, we tested the hypothesis that TGF $\beta$  may enhance the formation or function of these repressor complexes. In such a scenario, TGF $\beta$  would lead to a decreased transcriptional

activity in the absence of ligands, and PPAR $\beta/\delta$  agonists induce the dissociation of corepressors and their replacement with coactivators, thereby counteracting the TGF $\beta$  effect. Our data are consistent with this model: (i) the *NCOR2* gene (coding for SMRT) is a transcriptional

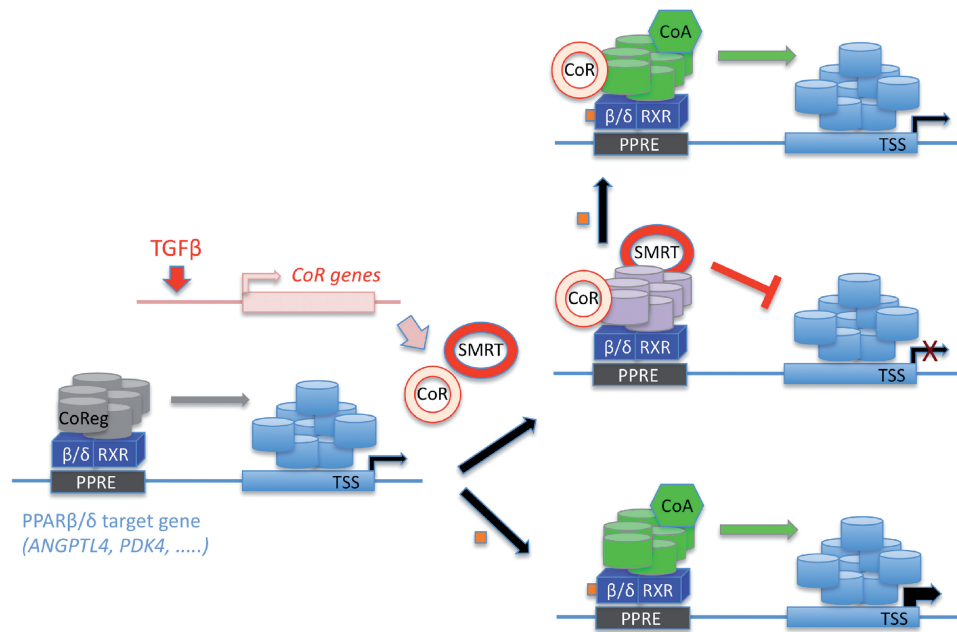


**Figure 8.** Model illustrating the repression of the PPAR $\beta/\delta$  target genes by TGF $\beta$  and its reversion by PPAR $\beta/\delta$  ligands. CoA, coactivator; CoR, corepressor; CoReg, activating or repressing coregulators; orange squares, synthetic PPAR $\beta/\delta$  ligand (GW501516). (Left) the absence of both GW501516 and TGF $\beta$  leads to a weak recruitment of positive and negative coregulators, resulting in a low rate of transcription. (Middle) TGF $\beta$  induces corepressor genes, including *NCOR2*, which leads to an enhanced recruitment of SMRT and other corepressors (CoR) to PPARE-bound PPAR $\beta/\delta$  complexes, and consequently an inhibition of transcription. (Bottom) GW501516 induces SMRT dissociation and favors the association with coactivators, leading to transcriptional activation. (Top) Other corepressors (CoR) induced by TGF $\beta$ , like those identified in Figure 6A, remain bound to the PPAR $\beta/\delta$ , resulting in a lower level of transcription compared to cells exposed to PPAR $\beta/\delta$  ligands in the absence of TGF $\beta$ .

target of TGF $\beta$  (Figure 6A and B); (ii) the TGF $\beta$ -induced *NCOR2* expression leads to an increased recruitment of the SMRT corepressor to the *ANGPTL4* PPAREs *in vivo* (Figure 6C); (iii) this enhancement of SMRT recruitment is markedly diminished by the PPAR $\beta/\delta$  agonist GW501516 (Figure 6C); (iv) the siRNA-mediated inhibition of *NCOR2* expression leads to a strong derepression of *ANGPTL4* transcription and an inhibition of TGF $\beta$ -mediated repression (Figure 7A and B); and (v) the same treatment also reduced the inducibility by PPAR $\beta/\delta$  ligands in the presence of TGF $\beta$  (Figure 7A and C). These findings provide compelling evidence for a functional link between the TGF $\beta$ -induced expression of SMRT, the impact of TGF $\beta$  on PPAR $\beta/\delta$  target genes and the counteracting effects of PPAR $\beta/\delta$  ligands. Importantly, similar siRNA effects were also observed with another class A gene, the PPAR $\beta/\delta$  target gene *PDK4* (Figures 4 and 7). This suggests that the regulatory mechanism identified here is not a peculiar feature of the *ANGPTL4* gene, but appears to have a broader relevance. Collectively, our findings establish a clear functional connection between the induction of corepressor expression by TGF $\beta$  and the transcription of PPAR $\beta/\delta$  target genes, as are illustrated by the model in Figure 8.

The data in Figure 7A and C indicate that after knockdown of *NCOR2* expression, TGF $\beta$  still represses *ANGPTL4* and *PDK4* transcription, albeit to a reduced extent. This suggests that SMRT may not be the only corepressor relevant in this context, and that the

PPAR $\beta/\delta$  repressor complex is probably subject to additional regulatory mechanisms triggered by TGF $\beta$ . This is supported by the observation that the overall expression level induced by PPAR $\beta/\delta$  ligands is higher than that observed after treatment with ligand plus TGF $\beta$  (Figure 4). Consistent with this hypothesis, TGF $\beta$  induces several other corepressor genes, such as *CALR* (calreticulin), *LCOR*, *MTA1*, *SHARP* and *SIN3B* (Figure 6A), which may play a role in the formation of PPAR $\beta/\delta$  repressor complexes, as previously published for *SHARP* (9,25–28). The clarification of these questions will be the subject of future studies aiming at a precise dissection of the molecular mechanism involved in the regulation of class A genes by PPAR $\beta/\delta$  and TGF $\beta$ .

#### Inhibition of TGF $\beta$ -mediated transcriptional activation by PPAR $\beta/\delta$ ligands

The genes represented by the second group are induced by TGF $\beta$ , which is diminished by PPAR $\beta/\delta$  agonists (Figure 2B, blue data points). This group contains several genes that are potentially relevant in view of the known function of PPAR $\beta/\delta$  in modulating the immune responses. One of these is interleukin-6, a cytokine with both pro-inflammatory and anti-inflammatory properties and a vast range of biological and pathophysiological activities, including a role in tissue fibrosis (33). Time course experiments suggest that repression of TGF $\beta$ -mediated *IL6* induction by PPAR $\beta/\delta$  ligands is a direct event, because it is detectable within 6h post-treatment (Figure 5C). The *IL6* gene is regulated by

multiple transcription factors, including NF $\kappa$ B and C/EBP, which have been suggested to interact with PPARs in different experimental systems (34,35). It is possible that the inhibitory effect of PPAR $\beta/\delta$  on TGF $\beta$ -induced *IL6* transcription is also associated with these transcription factors. Another potentially interesting gene in this context is *CD274* coding for B7-H1, a membrane-bound ligand that modulates the activation or inhibition of lymphocytes and myeloid cells (36). Taken together, these data suggest that in differentiating myofibroblasts PPAR $\beta/\delta$  agonists counteract the effects of TGF $\beta$  for a subset of target genes with functions in immune regulation, highlighting the relevance of these compounds as potential anti-fibrotic and anti-inflammatory drugs.

### Cooperative signaling by TGF $\beta$ and PPAR $\beta/\delta$

We also detected cooperation of the two signaling pathways for several genes (Supplementary Table S1; class C and D). The cooperatively repressed genes (class C) include the cell cycle and tumorigenesis promoting genes *KIT*, *FOXQ1* and *TOP2A*. This is of potential interest, because we observed cooperative effects of TGF $\beta$  and GW501516 also on cell-cycle regulation. Thus, GW501516 not only inhibited cell-cycle progression in untreated WI38 cells, but also enhanced the inhibitory effect of TGF $\beta$  (Figure S2). The cooperative regulation of genes that have been associated with the cell cycle may thus provide an explanation for the cooperation of GW501516 and TGF $\beta$  in the inhibition of cell-cycle progression. However, it cannot be ruled out at present that the cell-cycle effects mediated by the two ligands are functionally unrelated. Inhibition of cell proliferation by PPAR $\beta/\delta$  ligands has previously been reported for a number of other cell lines of different origins, but the underlying molecular mechanisms remain largely obscure (10).

### SUPPLEMENTARY DATA

Supplementary Data are available at NAR Online.

### FUNDING

The Deutsche Forschungsgemeinschaft (Mu601/12-1 and SFB/TR17); Genomics and Bioinformatics core facility of the LOEWE-Schwerpunkt 'Tumor and Inflammation'. Funding for open access charge: Research grant (DFG).

*Conflict of interest statement.* None declared.

### REFERENCES

1. Feige, J.N., Gelman, L., Michalik, L., Desvergne, B. and Wahli, W. (2006) From molecular action to physiological outputs: peroxisome proliferator-activated receptors are nuclear receptors at the crossroads of key cellular functions. *Prog. Lipid Res.*, **45**, 120–159.
2. Desvergne, B., Michalik, L. and Wahli, W. (2006) Transcriptional regulation of metabolism. *Physiol. Rev.*, **86**, 465–514.

3. Barish, G.D., Narkar, V.A. and Evans, R.M. (2006) PPAR $\delta$ : a dagger in the heart of the metabolic syndrome. *J. Clin. Invest.*, **116**, 590–597.
4. Forman, B.M., Tontonoz, P., Chen, J., Brun, R.P., Spiegelman, B.M. and Evans, R.M. (1995) 15-Deoxy-delta 12, 14-prostaglandin J2 is a ligand for the adipocyte determination factor PPAR gamma. *Cell*, **83**, 803–812.
5. Chinetti, G., Fruchart, J.C. and Staels, B. (2000) Peroxisome proliferator-activated receptors (PPARs): nuclear receptors at the crossroads between lipid metabolism and inflammation. *Inflamm. Res.*, **49**, 497–505.
6. Naruhn, S., Meissner, W., Adhikary, T., Kaddatz, K., Klein, T., Watzter, B., Müller-Brüsselbach, S. and Müller, R. (2010) 15-hydroxyicosatetraenoic acid is a preferential peroxisome proliferator-activated receptor  $\beta/\delta$  agonist. *Mol. Pharmacol.*, **77**, 171–184.
7. Chakravarthy, M.V., Lodhi, I.J., Yin, L., Malapaka, R.R., Xu, H.E., Turk, J. and Semenkovich, C.F. (2009) Identification of a physiologically relevant endogenous ligand for PPARalpha in liver. *Cell*, **138**, 476–488.
8. Michalik, L. and Wahli, W. (2007) Peroxisome proliferator-activated receptors (PPARs) in skin health, repair and disease. *Biochim. Biophys. Acta*, **1771**, 991–998.
9. Ricote, M. and Glass, C.K. (2007) PPARs and molecular mechanisms of transrepression. *Biochim. Biophys. Acta*, **1771**, 926–935.
10. Peters, J.M. and Gonzalez, F.J. (2009) Sorting out the functional role(s) of peroxisome proliferator-activated receptor- $\beta/\delta$  (PPAR $\beta/\delta$ ) in cell proliferation and cancer. *Biochim. Biophys. Acta*, **1796**, 230–241.
11. Kilgore, K.S. and Billin, A.N. (2008) PPAR $\beta/\delta$  ligands as modulators of the inflammatory response. *Curr. Opin. Investig. Drugs*, **9**, 463–469.
12. Müller, R., Rieck, M. and Müller-Brüsselbach, S. (2008) Regulation of cell proliferation and differentiation by PPAR $\beta/\delta$ . *PPAR Res.*, **2008**, 614852.
13. Peraza, M.A., Burdick, A.D., Marin, H.E., Gonzalez, F.J. and Peters, J.M. (2006) The toxicology of ligands for peroxisome proliferator-activated receptors (PPAR). *Toxicol. Sci.*, **90**, 269–295.
14. Müller-Brüsselbach, S., Kömhoff, M., Rieck, M., Meissner, W., Kaddatz, K., Adamkiewicz, J., Keil, B., Klose, K.J., Moll, R., Burdick, A.D. *et al.* (2007) Deregulation of tumor angiogenesis and blockade of tumor growth in PPAR $\beta$ -deficient mice. *EMBO J.*, **26**, 3686–3698.
15. Abdollahi, A., Schwager, C., Kleeff, J., Esposito, I., Domhan, S., Peschke, P., Hauser, K., Hahnfeldt, P., Hlatky, L., Debus, J. *et al.* (2007) Transcriptional network governing the angiogenic switch in human pancreatic cancer. *Proc. Natl Acad. Sci. USA*, **104**, 12890–12895.
16. Müller, R., Kömhoff, M., Peters, J.M. and Müller-Brüsselbach, S. (2008) A role for PPAR $\beta/\delta$  in tumor stroma and tumorigenesis. *PPAR Res.*, **2008**, 534294.
17. Ali, F.Y., Egan, K., FitzGerald, G.A., Desvergne, B., Wahli, W., Bishop-Bailey, D., Warner, T.D. and Mitchell, J.A. (2006) Role of prostacyclin versus peroxisome proliferator-activated receptor beta receptors in prostacyclin sensing by lung fibroblasts. *Am. J. Respir. Cell. Mol. Biol.*, **34**, 242–246.
18. Teunissen, B.E., Smeets, P.J., Willemsen, P.H., De Windt, L.J., Van der Vusse, G.J. and Van Bilsen, M. (2007) Activation of PPAR $\delta$  inhibits cardiac fibroblast proliferation and the transdifferentiation into myofibroblasts. *Cardiovasc Res.*, **75**, 519–529.
19. Lakatos, H.F., Thatcher, T.H., Kottmann, R.M., Garcia, T.M., Phipps, R.P. and Sime, P.J. (2007) The role of PPARs in lung fibrosis. *PPAR Res.*, **2007**, 71323.
20. Massague, J. (2008) TGF $\beta$  in cancer. *Cell*, **134**, 215–230.
21. Padua, D., Zhang, X.H., Wang, Q., Nadal, C., Gerald, W.L., Gomis, R.R. and Massague, J. (2008) TGF $\beta$  primes breast tumors for lung metastasis seeding through angiopoietin-like 4. *Cell*, **133**, 66–77.
22. Galaup, A., Cazes, A., Le Jan, S., Philippe, J., Connault, E., Le Coz, E., Mekid, H., Mir, L.M., Opolon, P., Corvol, P. *et al.* (2006) Angiopoietin-like 4 prevents metastasis through inhibition



- of vascular permeability and tumor cell motility and invasiveness. *Proc. Natl Acad. Sci. USA*, **103**, 18721–18726.
23. Desmouliere, A., Geinoz, A., Gabbiani, F. and Gabbiani, G. (1993) Transforming growth factor- $\beta$ 1 induces alpha-smooth muscle actin expression in granulation tissue myofibroblasts and in quiescent and growing cultured fibroblasts. *J. Cell. Biol.*, **122**, 103–111.
  24. Serini, G. and Gabbiani, G. (1996) Modulation of alpha-smooth muscle actin expression in fibroblasts by transforming growth factor- $\beta$  isoforms: an in vivo and in vitro study. *Wound Repair Regen.*, **4**, 278–287.
  25. Shi, Y., Hon, M. and Evans, R.M. (2002) The peroxisome proliferator-activated receptor  $\delta$ , an integrator of transcriptional repression and nuclear receptor signaling. *Proc. Natl Acad. Sci. USA*, **99**, 2613–2618.
  26. Lim, H.J., Moon, I. and Han, K. (2004) Transcriptional cofactors exhibit differential preference toward peroxisome proliferator-activated receptors  $\alpha$  and  $\delta$  in uterine cells. *Endocrinology*, **145**, 2886–2895.
  27. Krogsdam, A.M., Nielsen, C.A., Neve, S., Holst, D., Helledie, T., Thomsen, B., Bendixen, C., Mandrup, S. and Kristiansen, K. (2002) Nuclear receptor corepressor-dependent repression of peroxisome-proliferator-activated receptor  $\delta$ -mediated transactivation. *Biochem. J.*, **363**, 157–165.
  28. Semple, R.K., Meirhaeghe, A., Vidal-Puig, A.J., Schwabe, J.W., Wiggins, D., Gibbons, G.F., Gurnell, M., Chatterjee, V.K. and O'Rahilly, S. (2005) A dominant negative human peroxisome proliferator-activated receptor (PPAR)  $\alpha$  is a constitutive transcriptional corepressor and inhibits signaling through all PPAR isoforms. *Endocrinology*, **146**, 1871–1882.
  29. Massague, J., Blain, S.W. and Lo, R.S. (2000) TGF $\beta$  signaling in growth control, cancer, and heritable disorders. *Cell*, **103**, 295–309.
  30. Kaddatz, K., Adhikary, T., Finkernagel, F., Meissner, W., Müller-Brüsselbach, S. and Müller, R. (2010) Transcriptional profiling identifies functional interactions of TGF $\beta$  and PPAR $\beta/\delta$  signaling: synergistic induction of *ANGPTL4* transcription. *J. Biol. Chem.*, July 1, 2010 [Epub ahead of print; doi:10.1074/jbc.M110.142018].
  31. Boukamp, P., Petrussevska, R.T., Breitkreutz, D., Hornung, J., Markham, A. and Fusenig, N.E. (1988) Normal keratinization in a spontaneously immortalized aneuploid human keratinocyte cell line. *J. Cell. Biol.*, **106**, 761–771.
  32. Webber, M.M., Trakul, N., Thraves, P.S., Bello-DeOcampo, D., Chu, W.W., Storto, P.D., Huard, T.K., Rhim, J.S. and Williams, D.E. (1999) A human prostatic stromal myofibroblast cell line WPMY-1: a model for stromal-epithelial interactions in prostatic neoplasia. *Carcinogenesis*, **20**, 1185–1192.
  33. Kovalovich, K., DeAngelis, R.A., Li, W., Furth, E.E., Ciliberto, G. and Taub, R. (2000) Increased toxin-induced liver injury and fibrosis in interleukin-6-deficient mice. *Hepatology*, **31**, 149–159.
  34. Libermann, T.A. and Baltimore, D. (1990) Activation of interleukin-6 gene expression through the NF-kappa B transcription factor. *Mol. Cell. Biol.*, **10**, 2327–2334.
  35. Orjalo, A.V., Bhaumik, D., Gengler, B.K., Scott, G.K. and Campisi, J. (2009) Cell surface-bound IL-1 $\alpha$  is an upstream regulator of the senescence-associated IL-6/IL-8 cytokine network. *Proc. Natl Acad. Sci. USA*, **106**, 17031–17036.
  36. Keir, M.E., Butte, M.J., Freeman, G.J. and Sharpe, A.H. (2008) PD-1 and its ligands in tolerance and immunity. *Annu. Rev. Immunol.*, **26**, 677–704.